



OPEN Molecular insights into ulcerative colitis and orbital inflammation

Kang Tan^{1,3}, Pei Liu^{1,3}, Zixuan Wu¹, Xi Long¹, Yunfeng Yu¹, Pengfei Jiang^{2,4}✉ & Qinghua Peng^{1,4}✉

Ulcerative colitis (UC) is an increasingly prevalent inflammatory condition affecting the intestinal mucosa, while nonspecific orbital inflammation (NSOI) is a common non-neoplastic orbital disorder. Exploring the molecular interplay between UC and NSOI may help physicians make earlier diagnoses and enhance treatment approaches. We analyzed gene expression datasets (GSE58331, GSE105149, GSE206285, and GSE179285) for UC and NSOI from the GEO database. Using WGCNA and differential expression analysis, we identified genes commonly altered in both diseases. GO enrichment, PPI networks, and transcription factor prediction were performed using Cytoscape plugins (cytoHubba and iRegulon). Machine learning techniques were employed to assess transcription factor activity and evaluate potential therapeutic targets among the hub genes. We conducted an association analysis using the TwoSampleMR package in R to explore potential causal relationships between NSOI and UC. A total of 85 intersecting genes between NSOI and UC were identified, and enrichment analyses revealed their roles in immune and inflammatory processes. Key biomarkers, including CXCL10, CXCR4, CXCL9, CD27, SELL, MMP9, CD79A, CD3E, GZMK, and CCL19, were highlighted, linking them to processes such as leukocyte migration, viral response, and monocyte differentiation. STAT1 was identified as a shared transcription factor influencing both diseases. Machine learning algorithms identified eight potential genes for diagnostic and therapeutic use, with CXCL10 emerging as a key player in the pathogenesis of NSOI and UC. CXCL10 likely regulates CXCR4, LCK, CCR7, and other genes involved in pathways such as cytokine-cytokine receptor interactions, HIV-1 infection, and Epstein-Barr virus infection. This study offers insights into the co-pathogenic mechanisms of UC and NSOI, providing a foundation for further mechanistic research and therapeutic development.

Keywords Nonspecific orbital inflammation (NSOI), Ulcerative colitis (UC), Lasso regression, SVM-RFE, Autoimmune inflammatory disorder, Mendelian randomization

Abbreviations

NSOI	Nonspecific orbital inflammation
UC	Ulcerative colitis
GO	Gene Ontology
TCM	Traditional Chinese medicine
MF	Molecular functions
KEGG	Kyoto Encyclopedia of Genes and Genomes
GEO	Gene Expression Omnibus
BP	Biological processes
CC	Cellular components
DEGs	Differentially expressed genes

Non-specific orbital inflammation (NSOI), commonly known as orbital pseudotumor, is a benign, neoplastic, and non-infectious orbital inflammatory disease¹. This condition accounts for 8% to 11% of all orbital tumors, and is the third most common orbital disease in adults, after thyroid orbital disease and orbital lymphoma². NSOI mainly involves the lacrimal gland and usually occurs at age 30–60 years, especially in middle-aged women. Currently, the triggers involved in the pathogenesis of NSOI remain to be fully elucidated but have been reported to be associated with infection, autoimmune and systemic diseases, drugs, environmental factors, and individual characteristics^{3,4}. The dysregulation of the immune system is the major factor constituting the

¹Hunan University of Chinese Medicine, Changsha 410208, Hunan Province, China. ²Ophthalmology Center, Zhejiang Medical Health Quzhou Hospital, Quzhou 324004, Jiangsu Province, China. ³Kang Tan and Pei Liu contributed equally to this work. ⁴Pengfei Jiang and Qinghua Peng contributed equally to this work. ✉email: 619926567@qq.com; pqh410007@126.com

pathogenesis of NSOI⁵. The clinical diagnosis of NSOI is unclear, usually characterized by acute orbital signs and symptoms, and the pathophysiology remains unknown, increasing the difficulty of diagnosis and the uncertainty of treatment⁶. Clinically, the gold standard treatment for NSOI includes systemic corticosteroids, the use of NSAIDs, and immunosuppressive agents (calcineurin inhibitors and antiproliferative drugs)⁷, but its high costs, adverse reactions, and related complications. NSOI may lead to recurrent and refractory symptoms, causing considerable distress and complicating treatment.

Ulcerative colitis (UC) is a lifelong inflammatory disease characterized by alternating periods of exacerbation and remission⁸. It has become a global health problem, with a global prevalence of 5 million cases, and about 400 people per 100,000 people in North America are affected by UC, while its incidence is increasing worldwide⁹. The main manifestations of UC were abdominal colic, pus, mucous excretion, and bloody diarrhea. The pathogenesis of UC is not fully understood and is thought to be multifactorial, including genetic susceptibility, epithelial barrier defects, dysregulated immune response, and environmental factors¹⁰. Due to recurrent episodes of colonic inflammation, leading to chronic diarrhea and rectal bleeding, or extra-intestinal manifestations, leading to a reduced quality of life in UC patients. Meanwhile, UC increases the risk of colorectal cancer and reduces life expectancy. The diagnosis of UC is based on clinical, biological, endoscopic, and histological findings, but is clinically challenging and uncertain, especially in the early stage of the disease¹¹. Currently, the treatment method for UC is mainly to induce and maintain remission, using 5-aminosalicylic acid drugs, steroids, and immunosuppressive agents¹². Some patients may require a colectomy to treat drug-refractory disease or to treat colonic tumors¹³. Treatments for ulcerative colitis are expanding, and drugs with new targets offer hope for patients with moderate to severe UC. Based on the great challenges in UC diagnosis and treatment, it is urgent to explain the complex immune-inflammatory links of UC¹⁴. Through precise positioning of diagnostic markers, realize early detection and intervention, create targeted treatment methods, early detection and intervention, and realize the combination of precision therapy and personalized medicine¹⁵.

As a rare ocular manifestation of UC, NSOI has little knowledge of the mechanism of the disease and the optimal treatment^{16,17}. High-throughput data analysis is used in the diagnosis, prediction, and treatment of diseases. Through the analysis of patient genomic data and clinical data, the information on genomics, transcriptomics, and proteomics can be revealed, to help researchers understand the biological processes and disease occurrence mechanism of the human body¹⁸. Recent advances in bioinformatics have significantly contributed to a deeper understanding of UC, facilitating the identification of key molecular mechanisms, potential biomarkers, and therapeutic targets¹⁹. Genomic and transcriptomic analyses, including genome-wide association studies (GWAS) and RNA sequencing, have revealed several critical susceptibility genes, such as NOD2, IL23R, and ATG16L1, implicated in immune response and epithelial barrier dysfunction. These studies underscore the importance of immune and autophagy pathways in UC pathogenesis²⁰. Metagenomic and metabolomic profiling have illuminated the role of the gut microbiome and altered metabolic pathways in disease progression. Dysbiosis and changes in short-chain fatty acid (SCFA) production, particularly butyrate, have been linked to inflammation and epithelial damage²¹. Bioinformatics-driven integration of multi-omics data holds promise for identifying novel biomarkers and therapeutic approaches. Based on the rich NSOI and UC initiative high-throughput transcriptome sequencing data repository and detailed clinical annotations, we can deeply examine the transcriptional changes and related molecular pathways involving NSOI and UC, elucidate the common pathogenic mechanisms between these two diseases, and explore directions for future research. In pursuit of this, we performed an extensive bioinformatics analysis based on microarray datasets to identify the common hub genes, associated pathways, and transcription factors (TFs) of NSOI and UC (Fig. 1).

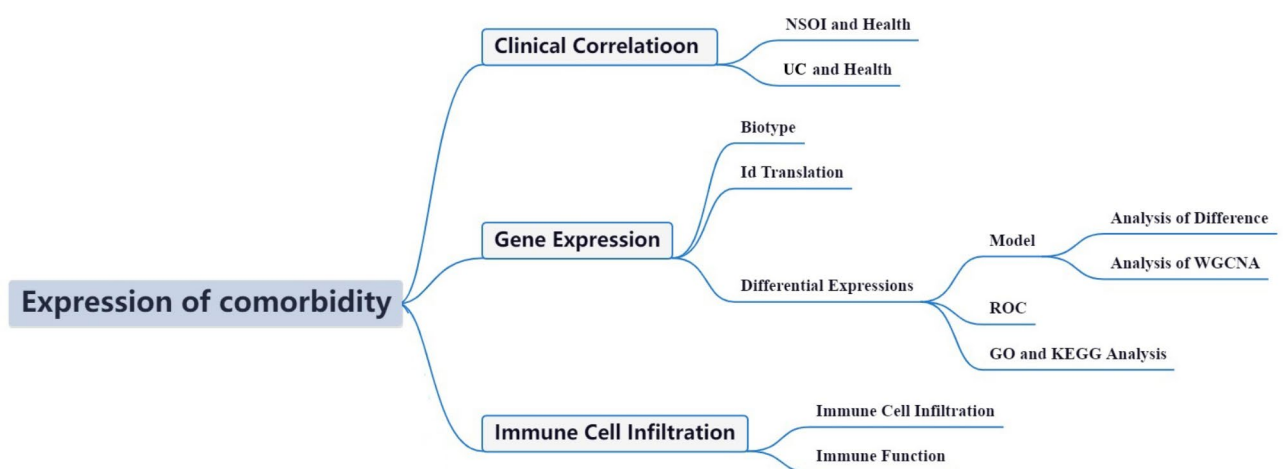


Fig. 1. Framework.

Materials and methods

We used the approaches proposed by Zi-Xuan Wu, et al. 2023²².

Data acquisition and preprocessing

We obtained the disease datasets from the GEO database. GSE58331 and GSE105149 were used to represent NSOI, supported by the GPL570-55999 platform. GSE206285 and GSE179285 were utilized for UC, using GPL13158 and GPL6480 platforms. Notably, GSE58331 and GSE206285 served as the training cohort, and GSE105149 and GSE179285 served as the test group. Data preparation was performed using R software (version 4.3.1). During pre-processing, we removed probes corresponding to multiple genes and used the platform's annotation file to convert probe IDs into gene symbols. In cases where multiple probes on the same gene are involved, we keep only the probe with the highest signal value. To ensure the consistency and reliability of the data, we have also taken measures to mitigate the potential impact of batch effects that are often introduced during the data centralization process. Batch effects, which arise from variations in experimental conditions, instrumentation, or sample processing over time or across different datasets, can significantly confound the interpretation of results. Therefore, limma, pheatmap, and ggplot2 packages were used to correct the data according to different groups (disease vs non-disease). The data were analyzed by taking log2. Finally, batchmat was performed on different groups of diseases for data batch calculation.

Transcriptomic data refinement and preprocessing

The probe-level expression matrices were converted into gene-level matrices by leveraging supplementary probe annotation files. For genes associated with multiple probes, the arithmetic mean of the corresponding probe values was used to represent the gene's expression. After this conversion, the datasets were standardized, followed by batch effect correction using the SVA package. The success of the normalization process was evaluated using principal component analysis (PCA). To identify DEGs between NSOI and control samples, we utilized the limma package (Linear Models for Microarray Data). Differentially expressed genes (DEGs) were defined as those with an absolute log fold change ($|\log FC|$) greater than 1 and an adjusted p -value less than 0.05, focusing on genes potentially linked to immune infiltration in NSOI and UC.

Enrichment analysis

To elucidate the biological implications and pathway associations of the differentially expressed genes (DEGs), we performed comprehensive Gene Ontology (GO) and Kyoto Encyclopedia of Genes and Genomes (KEGG) analyses. Using the R programming environment, we systematically explored the effects of differentially expressed protein-modifying genes (PMGs) on key biological processes (BP), molecular functions (MF), and cellular components (CC). This analysis aimed to uncover the underlying biological themes and molecular pathways influenced by these genes, providing a deeper understanding of their roles in disease pathogenesis and offering potential insights into novel therapeutic targets. Through this multifaceted approach, we sought not only to classify the DEGs but also to illuminate the intricate molecular interactions between NSOI and UC, thereby uncovering their broader biological and clinical significance. The analysis was conducted using the R software, leveraging tools such as the clusterProfiler, org.Hs.eg.db, enrichplot, and ggplot2 packages, with a focus on KEGG pathway data to enrich our interpretation. This integrated approach enabled us to capture the complexity of the molecular landscape associated with NSOI and UC, providing a comprehensive framework for further mechanistic exploration.

Identification of hub DEGs

To investigate the progression of NSOI and UC and to explore protein-coding gene interactions, we identified key hub genes from the DEGs and mapped their interactions using the STRING database. By integrating the results of weighted gene co-expression network analysis (WGCNA) with the DEGs, we constructed a protein-protein interaction (PPI) network, applying a stringent interaction score threshold of 0.7 to ensure the robustness of the identified relationships. WGCNA was used to investigate the relationship between gene expression patterns and disease traits, aiming to identify key gene modules associated with NSOI and UC. Gene expression data were first preprocessed to exclude low-quality genes and samples, removing those with low expression or minimal variance, as they provide limited insight into disease mechanisms. Data normalization was then performed to correct for systematic biases, ensuring sample comparability. A weighted adjacency matrix was constructed to represent pairwise gene relationships. Correlation coefficients were calculated and raised to a power (6 to 10) to generate a weighted similarity measure, which preserved both strong and weak correlations, offering a more precise depiction of gene co-expression compared to binary networks. A topological overlap matrix (TOM) was subsequently computed to assess the similarity between gene pairs, incorporating both direct co-expression and shared interactions within the network. Gene modules were identified through hierarchical clustering based on the TOM, grouping genes with highly correlated expression patterns. A dynamic tree-cutting algorithm was applied to segment the dendrogram into distinct modules, with the optimal number of modules determined by size and internal correlation. Finally, module eigengenes (ME)—the first principal component of each module—were correlated with clinical data to identify modules whose expression patterns were significantly associated with NSOI and UC, thereby revealing key biological processes and potential therapeutic targets. PPI network analysis was conducted in Cytoscape, leveraging the Molecular Complex Detection (MCODE) plug-in to uncover critical functional modules. To optimize module identification, MCODE parameters were set with a degree cutoff of 2, a maximum depth of 100, a node score cutoff of 0.2, and a K-core of 2. Genes identified through this approach were subjected to further in-depth analysis to assess their biological relevance. Additionally, we correlated the identified DEGs with clinical data to evaluate their potential clinical significance. This integrated

analysis not only provides a deeper understanding of the molecular interactions underpinning NSOI and UC but also highlights genes that may serve as potential biomarkers or therapeutic targets for these conditions.

Functional annotation via GO and KEGG pathway analyses

To understand the biological functions and signaling pathways associated with hub DEG expression profiles, comprehensive GO and KEGG pathway analyses were conducted using the R software environment. This analysis assessed how variations in hub gene expression affect BP, MF, and CC. We further examined the regulatory elements of hub genes through the TRRUST database, identifying transcription factors, which were visualized in Cytoscape, offering insight into the regulatory networks that may inform future therapeutic strategies for NSOI and UC. The analysis was conducted using the R software, leveraging tools such as the clusterProfiler, org.Hs.eg.db, enrichplot, and ggplot2 packages, with a focus on KEGG pathway data to enrich our interpretation.

Hub genes verification and transcription factor enrichment analysis (TRRUST)

For validation, we selected 156 genes from the common modules identified in our previous analyses and imported them into the STRING database to construct an additional protein–protein interaction (PPI) network. To further refine our identification of key hub genes, we utilized the cytoHubba plug-in in Cytoscape, applying five distinct algorithms—maximal clique centrality (MCC), maximum neighborhood component (MNC), closeness, radiality, and edge percolated component (EPC). These algorithms allowed for a comprehensive assessment of gene centrality, facilitating the identification and validation of the most influential hub genes within the network. Gene expression validation was performed using the GSE105149 dataset. To assess the normality of the data, we applied the Shapiro-Wilks test in R, confirming the normal distribution of gene expression values (W -value near 1, p -value > 0.05). T-tests were then conducted to compare gene expression levels between healthy controls and diseased states in both NSOI and UC, with statistical significance defined as $p < 0.05$. Finally, the validated hub genes were examined using the TRRUST database to identify their associated transcription factors. These regulatory interactions were visualized in Cytoscape, providing a comprehensive view of the transcriptional networks that may underlie the molecular mechanisms of NSOI and UC. This integrative approach not only strengthens the validity of our identified hub genes but also offers insights into the regulatory landscape of these diseases, highlighting potential therapeutic targets for future research.

Construction of integrated mRNA-miRNA-lncRNA regulatory networks and biomarker-immune infiltrate correlation analyses

Non-coding RNAs, particularly miRNAs and lncRNAs, play crucial roles in regulating gene expression. miRNAs primarily act post-transcriptionally by affecting mRNA stability and translation, while lncRNAs engage in diverse regulatory roles, including chromatin remodeling and transcriptional interference. This research examines the complex interactions between miRNAs and lncRNAs within the context of NSOI, with a focus on ceRNA networks. Target gene data for prominent miRNAs and lncRNAs were extracted from the miRTarbase and PrognScan databases. A comprehensive regulatory network integrating mRNA, miRNA, and lncRNA interactions, as well as their common targets in NSOI and UC, was constructed and visualized using Cytoscape. In addition, to further clarify the regulatory mechanisms of hub genes, a detailed gene regulatory network was created using GeneMANIA (<https://genemania.org/>). Spearman's rank correlation was used to analyze the relationships between diagnostic biomarkers and immune cell infiltration in the tissue microenvironment.

Mendelian randomization analysis

To ensure the independence of exposure and outcome variables in our genome-wide association study (GWAS) summary data, we engaged in an association analysis via the TwoSampleMR package in R. Designating STAT1-related expression as the exposure with UC and NSOI as the outcome, we aimed to explore potential causal relationships. The analysis entailed: 1. Instrumental Variables (IVs) Configuration: STAT1-related expressions were screened with a P -value threshold of $< 5 \times 10^{-8}$ to identify strongly associated exposures. 2. Independence Configuration: Linkage disequilibrium (LD) between SNPs was calculated using the PLINK clustering method, excluding SNPs with LD coefficient $r^2 > 0.001$ and within 10,000 kb to ensure SNP independence and reduce pleiotropic biases. 3. Statistical Strength Configuration: The robustness of instrumental variables was assessed using the F-statistic ($F = \beta^2 / SE^2$), with variables having $F < 10$ deemed inadequate to mitigate confounding effects.

Leveraging GWAS data, SNPs associated with the instrumental variables were identified, and through the “harmonise_data” function within TwoSampleMR, we aligned allelic directions of exposure and outcome, excluding incompatible SNPs. The inverse variance-weighted (IVW) method served as the cornerstone for causal inference, employing the variance of instrumental variables as weights to determine causal dynamics, thereby advancing our understanding of the genetic architecture underlying disease states.

Statistical considerations

Gene expression differences between distinct groups were statistically assessed using the gpubr package in R (version 4.3.1). For datasets that followed a normal distribution, independent two-sample t-tests were applied, while the Wilcoxon rank-sum test was used for data that did not meet normality assumptions. Statistical significance was determined by a p -value of less than 0.05 in all comparisons.

Results

DEG identification and principal component analysis

PCA successfully classified patients into risk-specific cohorts. Among the 644 DEGs in the NSOI, there were significant differences in some DEGs. Some genes clustered in the treatment group and others in the

control group. Treatment methods: CCR7, CD19, CCL19, CIITA, CXCR4, RHOH, TBC1D10C, CD52, CORO1A, TCL1A, DENND1C, etc. Control group: APOD, CRYAB, PPL, PPP1R1A, MAOA, CFH, C2orf40, TUBB2A, OGN, LYVE1, MAMDC2, etc. (Fig. 2a). In UC, among 1338 DEGs, there are significant differences in some DEGs. Additionally, some genes clustered in the treatment group, and some clustered in the control group. Treat: COL6A3, CYAT1, COL4A1, DERL3, MGC29506, IGLV6–57, IGLJ3, IGLV3–19, ELTD1, COL18A1, IGFBP5, SPON2, TIMP1, etc. Control: ADH1C, BMP3, VIPR1, HEPACAM2, MFSD4, PCK1, ISX, HAVCR1, IYD, LOC653602, ABCB1, etc. (Fig. 2b). We also intersected the differential genes of NSOI and UC, respectively. From here, it can be seen that there are 50 up-regulated genes and 35 down-regulated genes (Fig. 2c). Table S1–2).

Enrichment analysis of DEGs

The 85 intersecting genes were subjected to enrichment analysis. GO analysis identified 364 core targets distributed across BP, MF, and CC. In terms of MF, key functions were related to GTPase regulator activity (GO:0030695), nucleoside-triphosphatase regulator activity (GO:0060589), and actin-binding (GO:0003779). For CC, prominent components included the secretory granule lumen (GO:0034774), cytoplasmic vesicle lumen (GO:0060205), and the external side of the plasma membrane (GO:0009897). BP analysis highlighted leukocyte migration (GO:0050900), response to the virus (GO:0009615), and mononuclear cell differentiation (GO:1903131). Additionally, KEGG pathway enrichment analysis revealed that the over-expressed genes were primarily involved in pathways such as cytokine-cytokine receptor interaction (hsa04060), leukocyte transendothelial migration (hsa04670), and chemokine signaling (hsa04062) (Fig. 3; Table S3).

Hub DEG identification and clinical relevance analysis

We developed a PPI network to investigate the relationships among the 50 DEGs, as illustrated in Fig. 4. Using a strict interaction threshold of 0.7, key hub genes such as CXCL10, CXCR4, CXCL9, CD27, MMP9, CD79A, and SELL were identified (Fig. 5a, Table 1). Additionally, the MCODE plugin was employed to further divide and visualize critical subnetworks within the PPI network (Fig. 5b). The integrated calibration nomogram, which incorporated clinicopathological features of NSOI and UC along with the DEG-based prognostic model, demonstrated strong accuracy and potential therapeutic relevance for these conditions (Fig. 5c,d, Table S4).

Enrichment analysis of module DEGs

Through the PPI network, we also conducted a functional enrichment analysis of the screened module genes. GO enrichment analysis identified 411 core targets across BP, MF, and CC. For MF, significant terms included receptor ligand activity (GO:0048018), endopeptidase activity (GO:0004175), and G protein-coupled receptor binding (GO:0001664). CC terms primarily involved the external side of the plasma membrane (GO:0009897), plasma membrane signaling receptor complexes (GO:0098802), and late endosomes (GO:0005770). BP terms

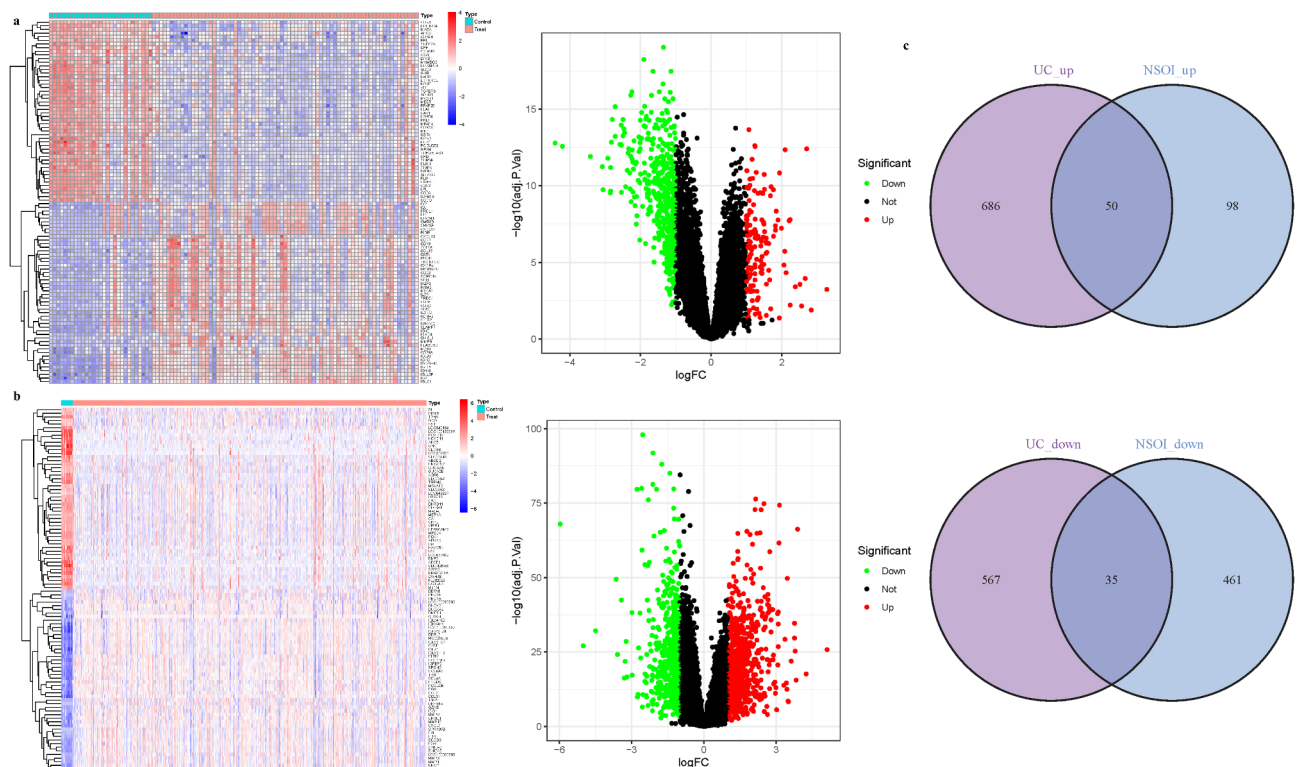


Fig. 2. Principal component analysis. (a) Heatmap and Volcano map of NSOI. (b) Heatmap and Volcano map of UC.

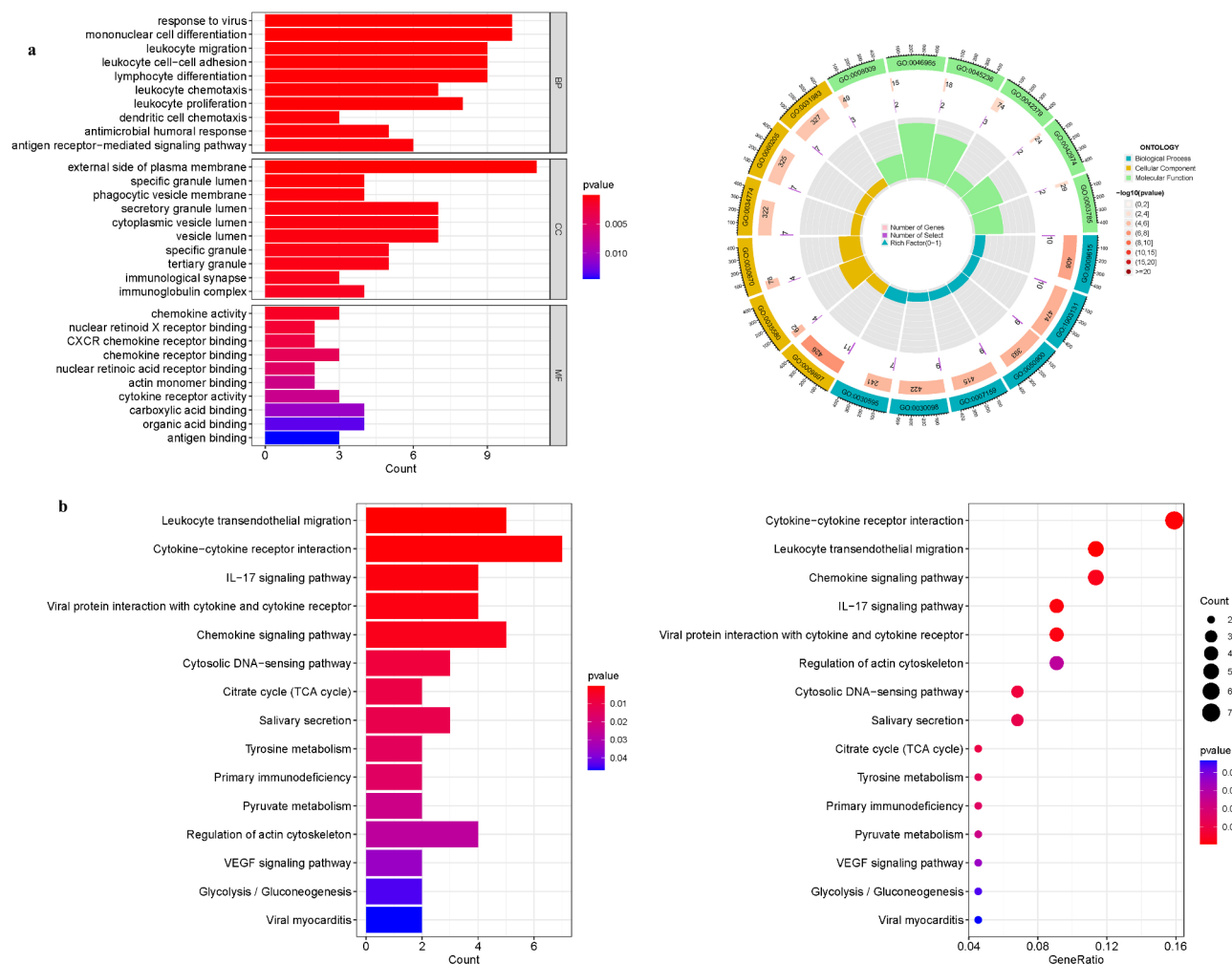


Fig. 3. For DEGs, GO, and KEGG analyses were performed. **(a)** GO enrichment; **(b)** KEGG enrichment. **(a)** Barplot graph for GO enrichment (the longer bar means the more genes enriched; q-value: the adjusted p-value). **(b)** Barplot graph for KEGG pathways (the longer bar means the more genes enriched);

highlighted immune response activation (GO:0002253), positive regulation of the MAPK cascade (GO:0043410), and cytokine-mediated signaling pathways (GO:0019221). KEGG pathway analysis revealed that the over-expressed genes were associated with pathways such as cytokine-cytokine receptor interaction (hsa04060), HIV-1 infection (hsa05170), Epstein-Barr virus infection (hsa05169), and the TNF signaling pathway (hsa04668) (Fig. 6, Table S5).

DEG identification and visualization

The GSE105149 dataset was utilized to validate the 10 selected modular genes. We visualized the expression of these 10 hub genes separately in the NSOI, UC, and normal sample groups (Figs. 7, 8).

Gene regulatory networks

To uncover the mechanisms driving these 10 genes, a comprehensive gene regulatory network was constructed (Fig. 9). Within this network, genes such as CXCL11, CD247, CD3D, CD3G, and CCL21 displayed significant interactions with the 10 hub genes, all of which are associated with inflammation and immune response. The detailed interactions within the network are outlined in Table S6. We hypothesize that these genes potentially contribute to the pathogenesis of UC and NSOI by modulating CXCL11, CD247, CD3D, CD3G, and CCL21, and associated downstream genes involved in immune and inflammatory pathways.

Identification of common RNAs and construction of miRNAs-LncRNAs shared genes network

We also examined three databases to identify 134 miRNAs and 165 lncRNAs linked to NSOI and UC (Tables S7a-b). By intersecting these miRNAs and lncRNAs with the shared genes, a miRNA-lncRNA-gene interaction network was built. Ultimately, the miRNA-gene network incorporated 123 lncRNAs, 129 miRNAs, and several overlapping genes, including 9 key hub genes: CXCR4, CXCL9, GZMK, SELL, MMP9, CXCL10, CD79A, CD27, and CD3E (Fig. 10).

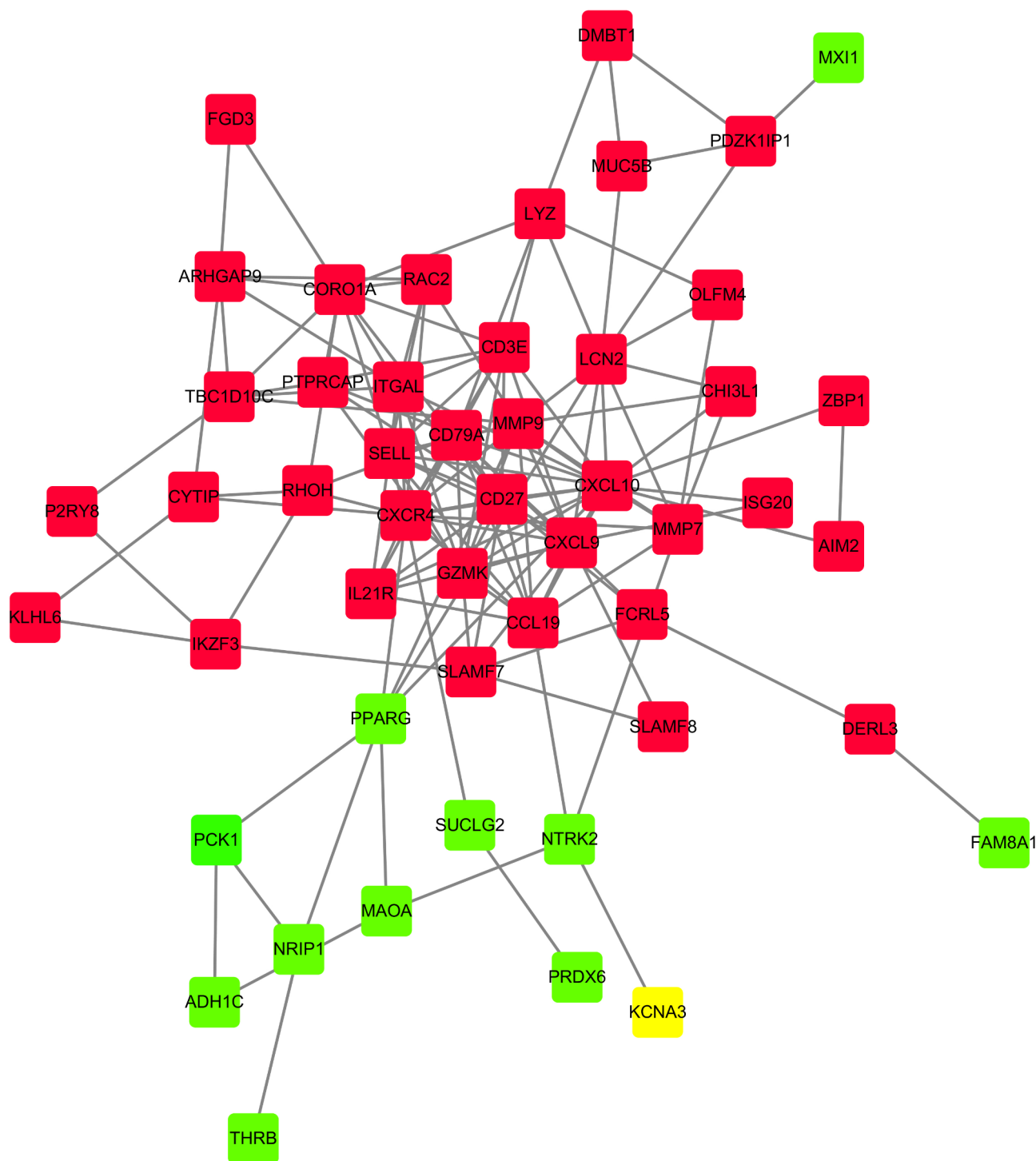


Fig. 4. PPI of Hub DEG.

Mendelian randomization analysis

In our exploration of the intrinsic connection between STAT1, NSOI, and UC forest plots were meticulously employed to visually articulate the associations. In the case of NSOI, SNPs rs13001419, and rs74511171 were all situated to the right of the confidence interval (Fig. 11b), suggesting a similar trend of association with NSOI. Further dissecting the heterogeneity inherent in our analysis, the funnel plot tailored to NSOI revealed a deviation from the expected symmetrical distribution, albeit maintaining a general symmetry. For UC, the SNP rs13001419 and rs74511171 conspicuously positioned themselves to the right of the confidence interval, indicating a positive association. Conversely, rs62143197 was observed to the left, reinforcing the credibility of our findings (Fig. 11a). This nuanced observation was further scrutinized through sensitivity analysis, employing a "leave-one-out" approach. Remarkably, the omission of any individual SNP from the analysis had

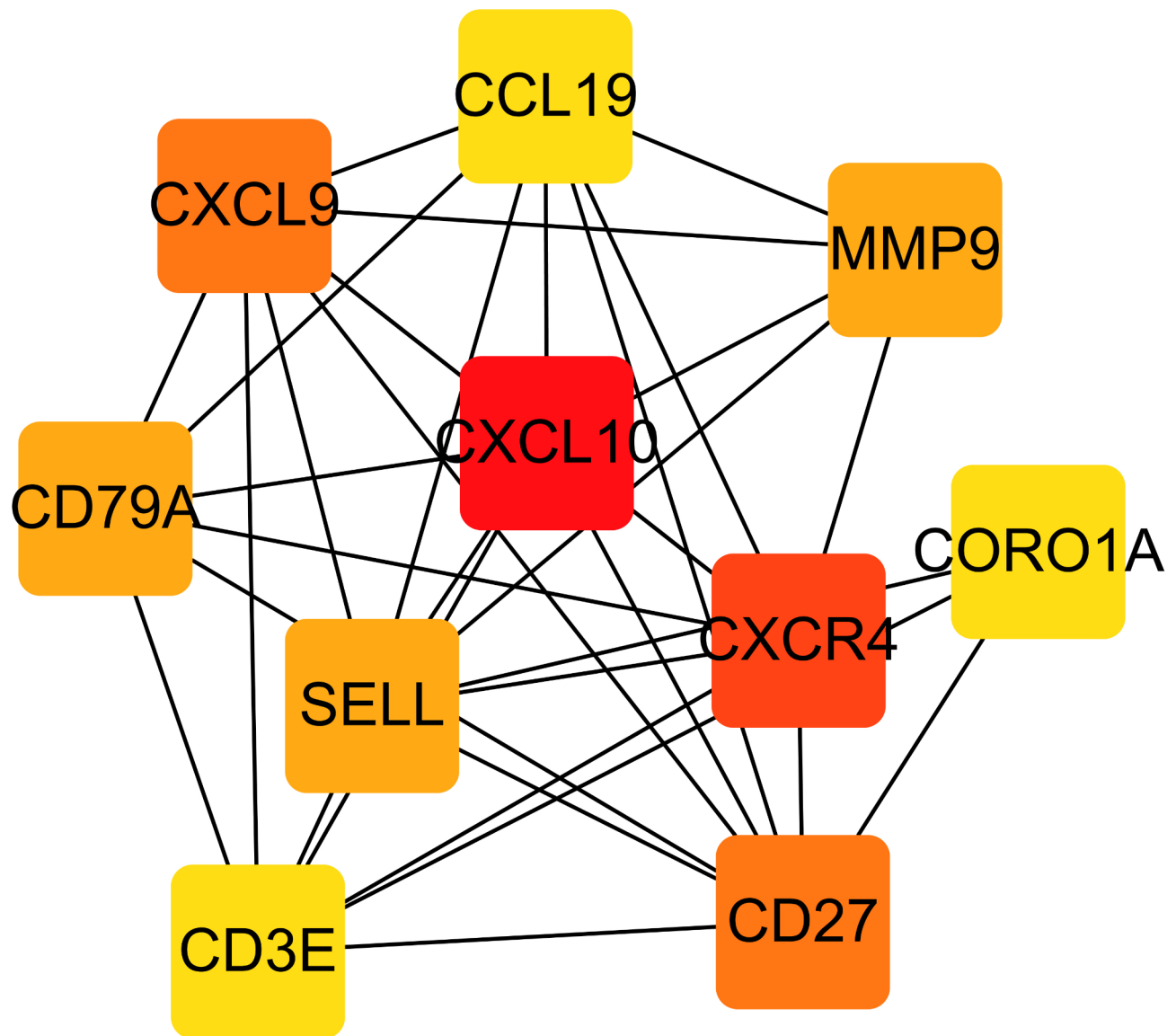


Fig. 5. (a) PPI network. (b) Module analysis network of PPI. (c) Calibration. (d) Nomogram.

a negligible effect on the results of the Inverse Variance Weighted (IVW) analysis, indicating that the remaining SNPs consistently mirrored the outcomes of the aggregate dataset. Substantiating the validity of our findings, the MR-Egger regression analysis was invoked, providing a solid foundation that bolsters both the robustness and authenticity of our results and the methodologies applied. This Mendelian randomization analysis unequivocally confirms the intimate association of STAT1 with NSOI and UC. Hence, it delineates a potential pathway to modulate the incidence, evolution, and progression of NSOI and UC by intervening in the functions of STAT1, presenting a promising avenue for therapeutic intervention and a deeper understanding of the disease mechanism.

Discussions

NSOI is a rare idiopathic eye disease with clinical manifestations ranging from extensive orbital signs to localized disease of specific orbital structures. This inflammation can lead to paralysis of the limiting eye muscles and double vision, which can lead to visual impairment²³. This visual deficiency may result from exposure keratopathy, optic nerve compression, posterior scleritis, or compartment syndrome. The molecular basis is still unclear, but there is growing evidence that changes in gene expression are crucial²⁴. UC is an idiopathic chronic inflammatory disease of the colon mucosa that begins in the rectum and usually extends continuously to the proximal end through part or the entire colon²⁵. Bloody diarrhea is the characteristic symptom of the disease. NSOI is a rare ophthalmic manifestation of UC, and little is known about the comorbidity mechanism and relationship between the two. Evidence suggests a complex interaction between inflammation and carcinogenic pathways that may facilitate connections between common molecular signals of inflammation and cell damage²⁶.

node_name	MCC	DMNC	MNC	Degree	Closeness	Betweenness
CXCL10	2710	0.48461	16	18	31.41667	428.35415
CXCR4	1967	0.43064	15	16	30.5	489.6309
CXCL9	2416	0.47297	14	14	28.75	206.40442
CD27	2464	0.52927	14	14	28.75	191.7128
SELL	1602	0.60003	12	12	27.33333	42.8271
MMP9	313	0.47511	11	12	28.28333	189.92333
CD79A	1110	0.43905	12	12	27.75	189.12403
CD3E	778	0.55995	11	11	26.91667	52.61123
GZMK	750	0.54298	11	11	26.41667	40.29222
CCL19	1946	0.57691	11	11	27.08333	123.8757
CORO1A	55	0.33919	10	11	25.48333	153.90686
LCN2	42	0.34989	8	10	26.45	347.89897
ITGAL	288	0.47886	10	10	26.08333	72.44562
MMP7	52	0.37904	8	8	24.95	103.15584
PPARG	15	0.47366	4	7	25.03333	421.24446
IL21R	1440	0.73175	7	7	24.25	0.25
LYZ	7	0.30898	3	6	23.5	136.14459
PTPRCAP	32	0.42794	6	6	21.85	12.5287
SLAMF7	11	0.32413	5	6	22.31667	84.14032

Table 1. Analysis results of key genes screened by MCODE.

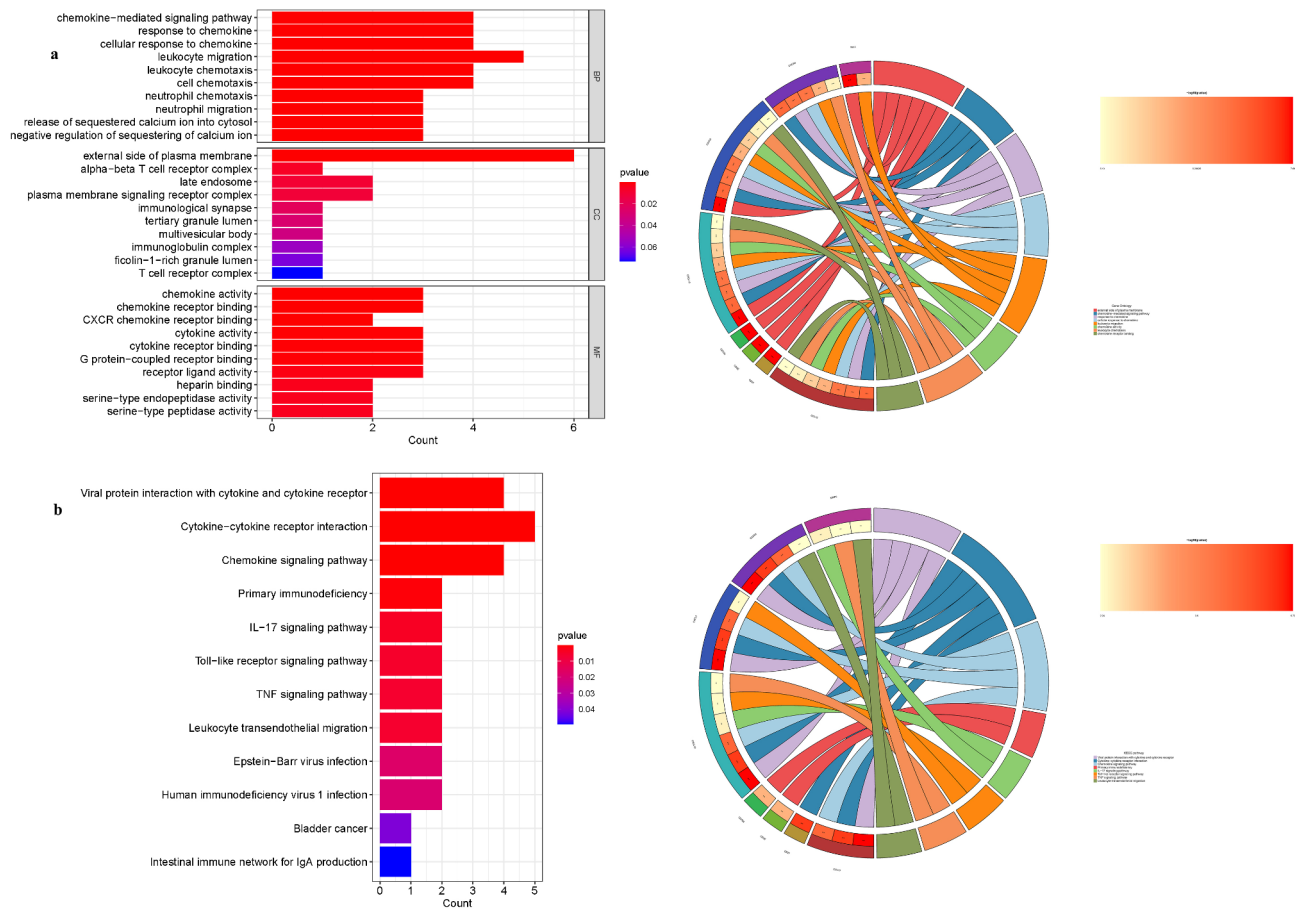


Fig. 6. For DEGs, GO, and KEGG analyses were performed. (a) GO enrichment; (b) KEGG enrichment. (a) Barplot graph for GO enrichment (the longer bar means the more genes enriched; q-value: the adjusted p-value). (b) Barplot graph for KEGG pathways (the longer bar means the more genes enriched);

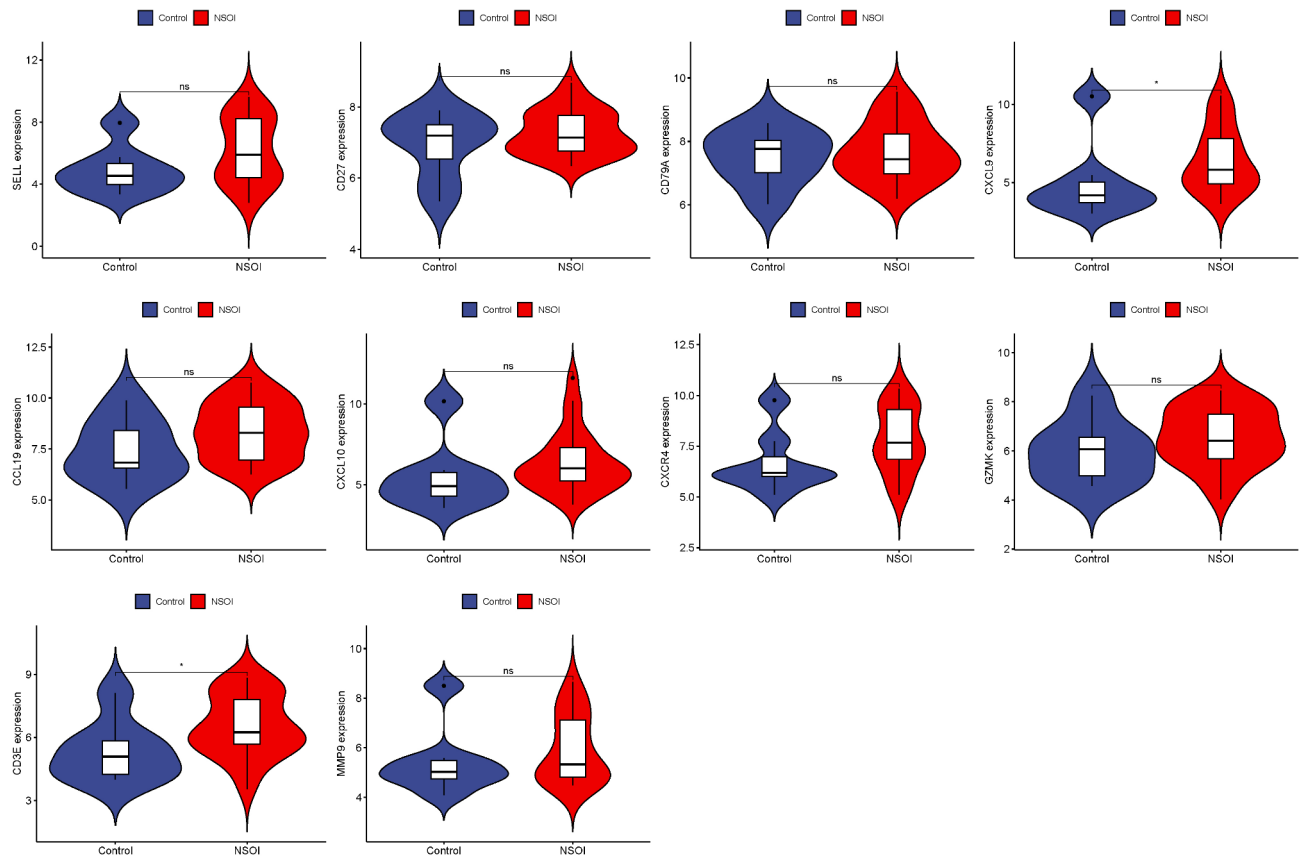


Fig. 7. All hub genes are co-expressed in the same line plot of NSOI.

Exploring these connections may therefore uncover new dimensions of pathophysiology between NSOI and UC, which could aid in the clinical diagnosis and treatment of disease. Through a detailed exploration of the cytokine profiles and genetic markers shared by these two diseases, the key to their simultaneous expression is elucidation, laying the foundation for precise medical strategies for challenging eye diseases.

We first identified gene modules co-expressed in both NSOI and UC, leading to the discovery of 85 genes. GO and KEGG enrichment analyses were conducted to explore the shared biological functions and pathways, revealing that both NSOI and UC are closely linked through inflammatory and immune responses, likely key mechanisms connecting these conditions. Previous studies have also associated NSOI with streptococcal infections, viral respiratory illnesses, and autoimmune diseases such as rheumatologic disorders, multifocal fibrosis, and Crohn's disease^{27–29}. UC is a chronic inflammatory disease affecting the colon, characterized by persistent inflammation of the colonic mucosa, with immune responses and inflammatory mediators playing a critical role in its pathogenesis. Immune cell trafficking is a key factor in intestinal immune responses, both in maintaining homeostasis and in the pathological conditions associated with UC³⁰. This process involves adhesion molecules, chemotactic factors, and receptors expressed on the surfaces of immune cells, vasculature, and stromal gut tissues, as well as the related signaling pathways. The TNF and IL-17 signaling pathways identified in the KEGG enrichment analysis establish a connection between NSOI and UC. TNF signaling is strongly implicated in a range of ocular conditions, including dry eye, uveitis, and macular edema^{31–33}. TNF is a potent pro-inflammatory cytokine that induces the activation of downstream signaling molecules such as NF- κ B, leading to the expression of inflammatory mediators. These mediators contribute to the disruption of the blood-retinal barrier, immune cell infiltration, and the promotion of angiogenesis and apoptosis in retinal cells. IL-17, primarily produced by Th17 cells, also plays a pivotal role in ocular inflammation. It amplifies the inflammatory cascade by stimulating the production of pro-inflammatory cytokines, chemokines, and matrix metalloproteinases (MMPs), thereby exacerbating tissue damage and contributing to disease progression in conditions such as uveitis and keratitis. Similarly, in UC, both TNF and IL-17 are key drivers of the chronic inflammatory environment. Elevated TNF levels are characteristic of UC, promoting apoptosis of intestinal epithelial cells, increasing gut barrier permeability, and recruiting inflammatory cells to the colonic mucosa. TNF inhibitors have been widely used as therapeutic agents in UC, underscoring the critical role of this cytokine in the disease's pathology¹². Although IL-17 was initially thought to have a protective role in mucosal immunity, it has been shown to contribute to UC pathogenesis³⁴. Which is by promoting neutrophil recruitment and enhancing the production of inflammatory cytokines, including IL-6 and TNF. Through the STRING database, we identified protein interaction relationships and ultimately identified 10 hub genes: CXCL10, CXCR4, CXCL9,

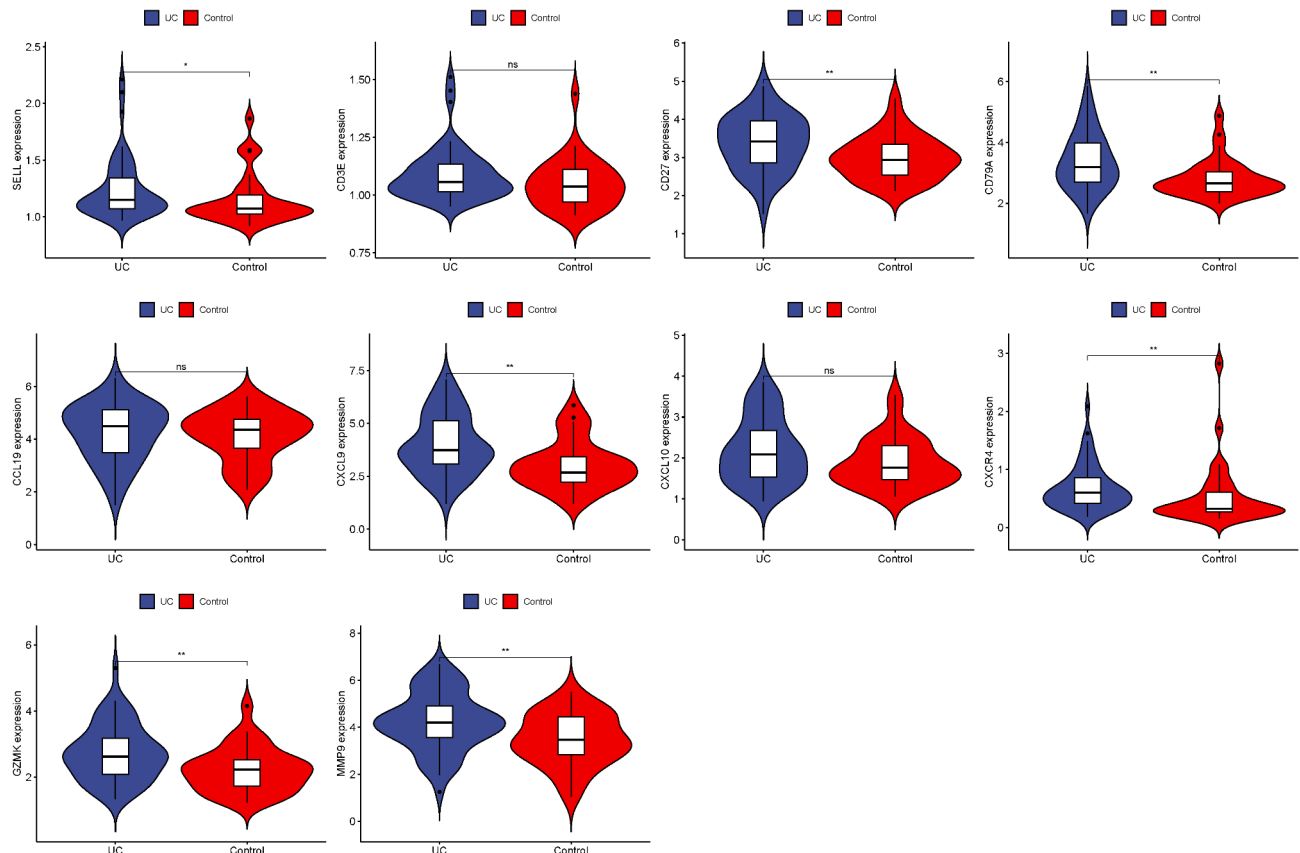


Fig. 8. All hub genes are co-expressed in the same line plot of UC.

CD27, SELL, MMP9, CD79A, CD3E, GZMK, and CCL19. Validation results from external datasets also indicated that these 4 hub genes have high diagnostic value.

STAT1 is a key transcription factor involved in the immune response, particularly in the regulation of inflammation. It plays a pivotal role in mediating the effects of interferons and is critical for the activation of numerous immune pathways, including those associated with autoimmunity and chronic inflammatory diseases³⁵. STAT1 has been implicated in the pathogenesis of UC, a chronic inflammatory bowel disease (IBD) characterized by relapsing inflammation of the colon and rectum. In UC, STAT1 activation is thought to exacerbate the inflammatory response, promoting the production of pro-inflammatory cytokines and chemokines that drive the inflammatory cascade³⁶. Dysregulated STAT1 signaling contributes to the persistence of inflammation, disrupting mucosal homeostasis and leading to the destruction of the intestinal epithelium. In the context of ocular diseases, including conditions such as uveitis and other forms of ocular inflammation, STAT1 also plays a critical role³⁷. STAT1 has been shown to be upregulated in ocular tissues during inflammatory responses, particularly in diseases with an autoimmune or inflammatory etiology. Its activation in the eye can lead to the induction of inflammatory cytokines and the recruitment of immune cells, contributing to tissue damage and exacerbating disease progression³⁸. In autoimmune forms of uveitis, such as those associated with IBD, including UC, the dysregulation of STAT1 signaling may promote the cross-talk between systemic inflammation and ocular immune responses, potentially increasing the risk of ocular manifestations³⁹. Thus, STAT1 represents a critical molecular link between UC and ocular inflammation, suggesting that its dysregulation may not only drive the chronic intestinal inflammation characteristic of UC but also extend its pathological effects to the eye. Targeting STAT1 signaling pathways could offer potential therapeutic avenues for both UC and associated ocular complications, underscoring the importance of this transcription factor in the broader context of autoimmune and inflammatory diseases.

The genes CXCL10, CXCR4, CXCL9, CD27, and SELL encode molecules that are integral to immune regulation and metabolic processes. These chemokines and immune markers are crucial for modulating immune responses in both ocular diseases and UC, underscoring their central role in inflammation and immune cell migration⁴⁰. In ocular diseases such as dry eye and ocular sarcoidosis, CXCL10 and CXCL9 are highly expressed and drive the recruitment of immune cells to inflamed tissues^{41,42}. CXCL10, typically induced by IFN- γ , binds to CXCR3 and promotes the migration of Th1 cells, intensifying inflammation. Similarly, CXCL9 recruits activated T cells, exacerbating local inflammatory responses. CXCR4, a receptor involved in hematopoietic and immune cell migration, contributes to the pathogenesis of retinal diseases like age-related macular degeneration (AMD) by regulating angiogenesis and inflammation, mediating monocyte and endothelial cell migration to sites of inflammation, and worsening tissue damage⁴³. CD27, a marker of memory T cells, plays a significant role

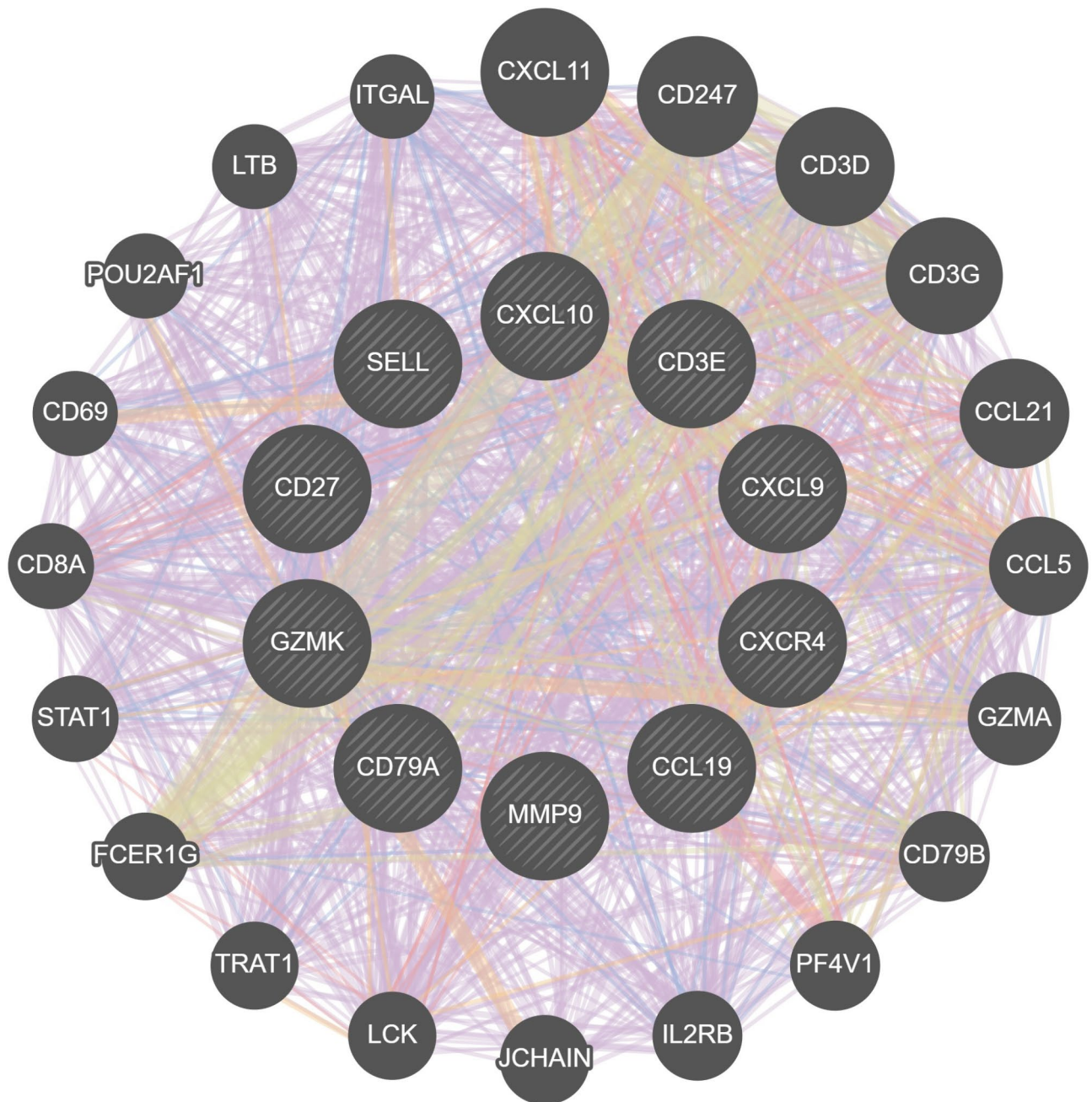


Fig. 9. Gene regulatory networks of these 10 genes.

in sustaining chronic inflammation in autoimmune eye conditions, such as uveitis, by promoting prolonged immune activation⁴⁴. SELL, or L-selectin, aids in the homing and migration of naive and central memory T cells into lymphoid and inflamed tissues, including the eye, thereby enhancing the recruitment of immune cells and local inflammation⁴⁵. In UC, CXCL10 and CXCL9 are also upregulated, driving the recruitment of effector T cells to the inflamed colonic mucosa⁴⁶. Their interaction with CXCR3-expressing cells facilitates the infiltration of Th1 and cytotoxic T lymphocytes, contributing to epithelial damage. CXCR4 plays a pivotal role in guiding immune cells to the gut, influencing mucosal immune responses, and exacerbating inflammation by promoting neutrophil and T-cell trafficking⁴⁷. CD27 perpetuates chronic inflammation in UC by maintaining the activation of memory T cells, particularly in sustaining Th1 and Th17 responses⁴⁸. SELL further contributes to the trafficking of lymphocytes into inflamed colonic tissues, aggravating mucosal inflammation and chronic immune activation⁴⁹. The dysregulation of CXCL10, CXCL9, CXCR4, CD27, and SELL in both ocular diseases and UC underscores their importance in immune cell recruitment, retention, and activation, driving prolonged inflammation and tissue damage. These molecules serve as potential therapeutic targets for modulating immune responses and reducing inflammation in these inflammatory conditions. Collectively, they illustrate the intricate

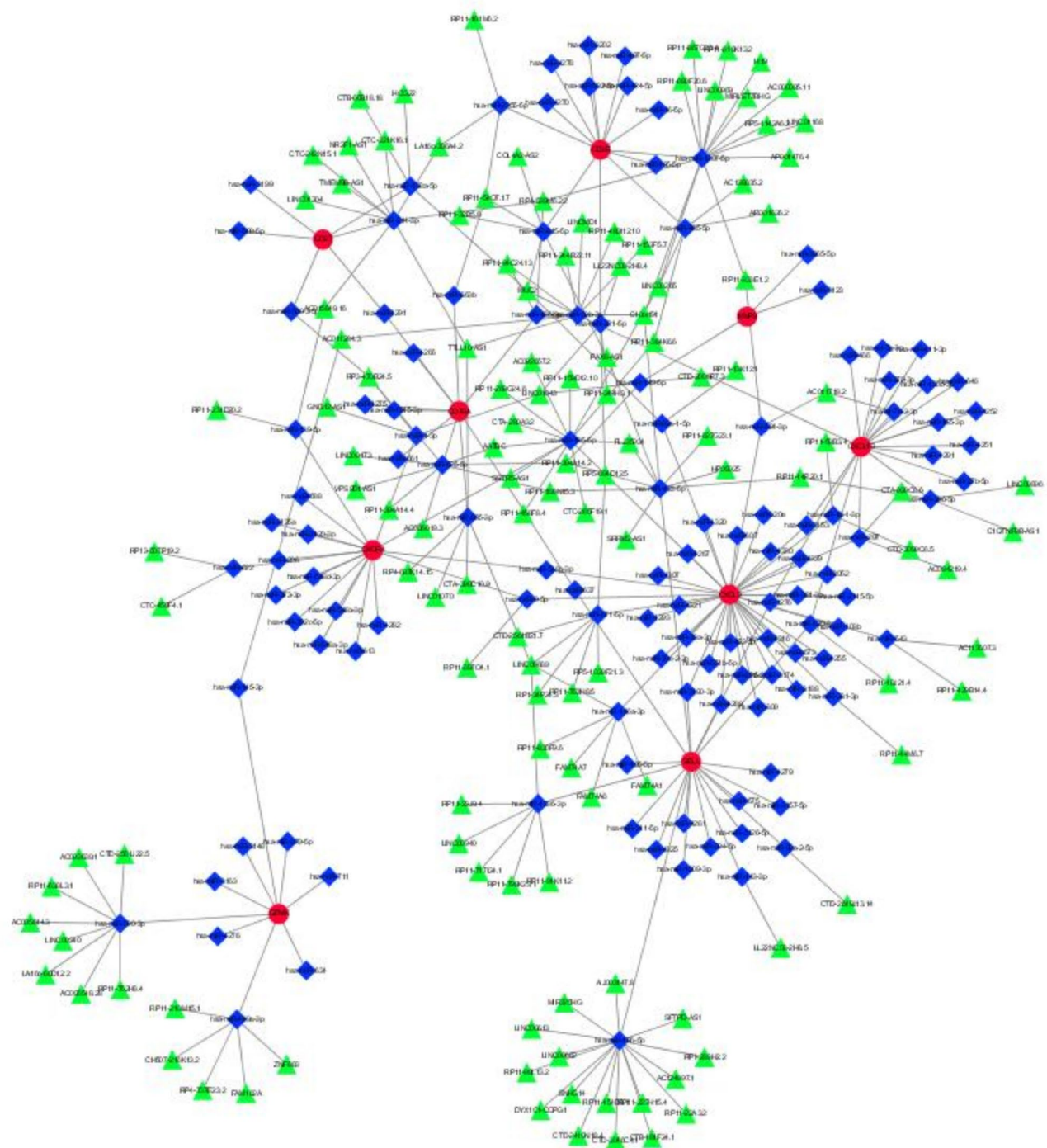


Fig. 10. miRNAs-LncRNAs shared Genes Network. Note: Red circles are mRNAs, blue quadrangles are miRNAs, and green triangles are lncRNAs.

connections between local ocular pathology and systemic disease, highlighting the intertwined nature of immune and metabolic responses in health and disease.

The exploration of biomarkers in the context of NSOI and UC has been markedly scant, with the nexus between metabolic processes and ocular diseases only recently beginning to unfurl through bioinformatics analyses^{50–52}. In this emerging field, Liu et al. have delineated hub genes associated with NSOI using Weighted Gene Coexpression Network Analysis, while Hu et al. have crafted a bioinformatics model for thyroid eye disease, identifying 11 pivotal genes including ATP6V1A and PTGES3 among others. Despite the clinical association between NSOI and UC, research on their shared biomarkers remains limited. Our study represents a pioneering effort to explore the relatively under-investigated intersection between these two conditions. While existing research largely relies on bioinformatics to uncover the connections between immune responses and

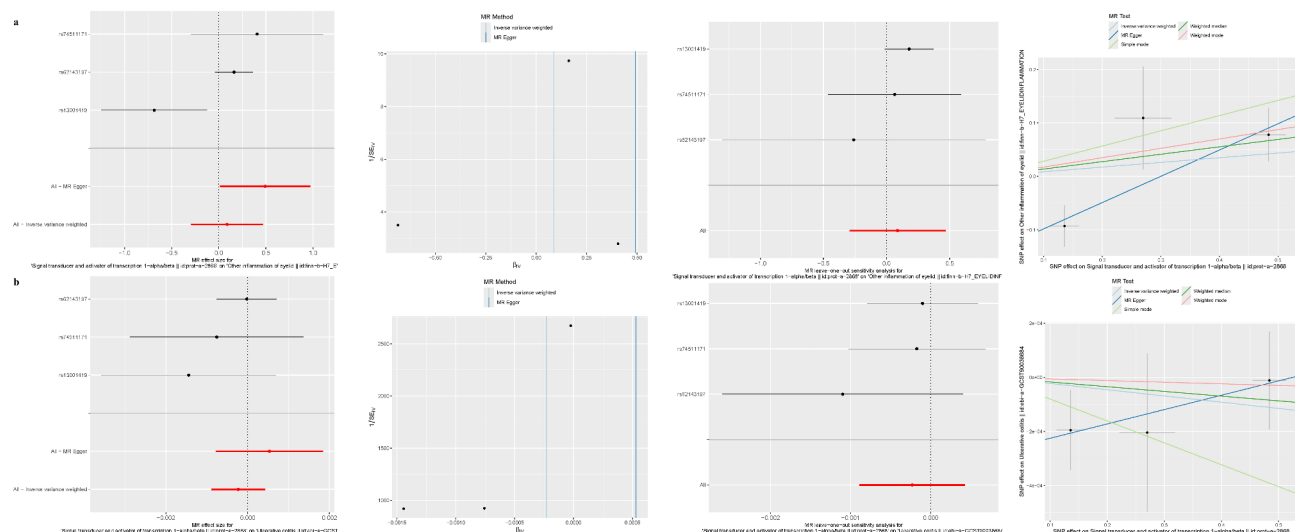


Fig. 11. Mendelian randomization analysis. (a) NSOI. (b) UC.

ocular diseases, the mechanisms underlying the comorbidity of eye diseases and related systemic conditions, such as UC, remain insufficiently explored. This work distinguishes itself by proposing a novel framework for understanding the comorbidity between NSOI and UC, with implications for guiding therapeutic strategies. Our approach aims to facilitate early diagnosis and targeted treatment of UC in patients with NSOI. The validity of our findings is supported by a robust dataset derived from the GEO, which provides a strong analytical foundation for the insights generated. However, despite the theoretical and methodological advances presented in our study, several limitations must be acknowledged. Although we employed comprehensive bioinformatics techniques and validated our results using external gene expression profiles, the analysis remains largely exploratory. Additional empirical studies are required to further substantiate our findings and establish a solid theoretical framework for future investigations in this field.

Conclusions

This study provides the first comprehensive investigation of overlapping hub genes, pathways, and transcription factors in the peripheral blood of patients with NSOI and UC. We identified key genes, such as CXCL10, CXCR4, CXCL9, CD27, and SELL, along with significant pathways, including TNF and IL-17 signaling. These discoveries offer important insights into the common pathogenic mechanisms underlying both NSOI and UC, contributing to a deeper understanding of these complex disorders.

Data availability

The datasets generated during and/or analyzed during the current study are available in the GEO repository, <https://www.ncbi.nlm.nih.gov/geo/>, GSE58331, GSE105149, GSE58331, and GSE105149.

Received: 27 September 2024; Accepted: 4 February 2025

Published online: 28 February 2025

References

- Eshraghi, B., Sonbolestan, S. A., Abtahi, M. A. & Mirmohammadsadeghi, A. Clinical characteristics, histopathology, and treatment outcomes in adult and pediatric patients with nonspecific orbital inflammation. *J. Curr. Ophthalmol.* **31**, 327–334. <https://doi.org/10.1016/j.joco.2019.03.004> (2019).
- Jonathan, E. L. et al. Epidemiology of orbital inflammatory disease: An AAO IRIS registry study. *Ocul. Immunol. Inflamm.* <https://doi.org/10.1080/09273948.2024.2322013> (2024).
- Anna, M. S. Histopathologic clues to the etiopathogenesis of orbital inflammatory disease: Idiopathic, IgG4-related, neoplastic, autoimmune and beyond. *Semin. Diagn. Pathol.* <https://doi.org/10.1053/j.semdp.2024.01.011> (2024).
- Edward, J. W. et al. Neutrophil-to-lymphocyte ratios distinguish idiopathic orbital inflammation from orbital infectious disease. *Ophthalmic Plastic Reconstr. Surg.* <https://doi.org/10.1097/iop.00000000000002519> (2023).
- Wu, K. Y., Kulbay, M., Daigle, P., Nguyen, B. H. & Tran, S. D. Nonspecific orbital inflammation (NSOI): Unraveling the molecular pathogenesis, diagnostic modalities, and therapeutic interventions. *Int. J. Mol. Sci.* **25**, 1553. <https://doi.org/10.3390/ijms25031553> (2024).
- Min Joung, L. et al. Non-specific orbital inflammation: Current understanding and unmet needs. *Prog. Retinal Eye Res.* <https://doi.org/10.1016/j.preteyeres.2020.100885> (2021).
- Vasiliki, T. et al. P119 Characteristics and treatment of fibrosclerosing orbital inflammatory disease. *Rheumatology* <https://doi.org/10.1093/rheumatology/keaa111.117> (2020).
- Eisenstein, M. Ulcerative colitis: Towards remission. *Nature* **563**, S33. <https://doi.org/10.1038/d41586-018-07276-2> (2018).
- Ungaro, R., Mehandru, S., Allen, P. B., Peyrin-Biroulet, L. & Colombel, J. F. Ulcerative colitis. *Lancet* **389**, 1756–1770. [https://doi.org/10.1016/s0140-6736\(16\)32126-2](https://doi.org/10.1016/s0140-6736(16)32126-2) (2017).
- Le Catherine, B., Sailish, H. & Laurent, P. B. Ulcerative colitis. *Lancet* [https://doi.org/10.1016/s0140-6736\(23\)00966-2](https://doi.org/10.1016/s0140-6736(23)00966-2) (2023).
- Beatriz, G. & Gilaad, G. K. Ulcerative colitis in adults. *JAMA* <https://doi.org/10.1001/jama.2023.15389> (2023).

12. Ariela, H. & Siddharth, S. Expanding targeted immune modulators in ulcerative colitis. *Lancet* [https://doi.org/10.1016/s0140-6736\(21\)00891-6](https://doi.org/10.1016/s0140-6736(21)00891-6) (2021).
13. Neurath, M. F. & Leppkes, M. Resolution of ulcerative colitis. *Semin. Immunopathol.* **41**, 747–756. <https://doi.org/10.1007/s00281-019-00751-6> (2019).
14. Evelyn Calderon, M., Christian, Z.-D., Wern Lynn, N., Seema Sharma, G. & Maria, J. Assessment of the immune cell landscape in inflammatory bowel disease. *Gastroenterology* <https://doi.org/10.1053/j.gastro.2023.03.092> (2023).
15. Zhu, Y. et al. CXCL8 chemokine in ulcerative colitis. *Biomed. Pharmacother.* **138**, 111427. <https://doi.org/10.1016/j.biopha.2021.111427> (2021).
16. Kevin, P. et al. S2757 Eye-BD—A rare case of orbital myositis as an extra-intestinal manifestation of Crohn's disease. *Am. J. Gastroenterol.* <https://doi.org/10.14309/01.ajg.0000867668.38798.5e> (2022).
17. Pejman, R. et al. Ocular complications of pediatric inflammatory bowel disease: A case series from a pediatric tertiary medical center. *Clin. Pediatr.* <https://doi.org/10.1177/00099228221078105> (2022).
18. Rossin, E. et al. Analysis of immune checkpoint blockade biomarkers in elderly patients using large-scale cancer genomics data. *J. Clin. Oncol.* https://doi.org/10.1200/jco.2021.39.15_suppl.2543 (2021).
19. Xu, M. et al. Identification of immune-related gene signature and prediction of CeRNA network in active ulcerative colitis. *Front Immunol.* **13**, 855645. <https://doi.org/10.3389/fimmu.2022.855645> (2022).
20. Yang, Y. et al. Biomarkers prediction and immune landscape in ulcerative colitis: Findings based on bioinformatics and machine learning. *Comput. Biol. Med.* **168**, 107778. <https://doi.org/10.1016/j.compbiomed.2023.107778> (2024).
21. Ohkusa, T. et al. Comparison of the gut microbiota of patients who improve with antibiotic combination therapy for ulcerative colitis and those who do not: Investigation by fecal metagenomic analyses. *Nutrients* **16**, 3500. <https://doi.org/10.3390/nu16203500> (2024).
22. Wu, Z. et al. A novel Alzheimer's disease prognostic signature: Identification and analysis of glutamine metabolism genes in immunogenicity and immunotherapy efficacy. *Sci. Rep.* **13**, 6895. <https://doi.org/10.1038/s41598-023-33277-x> (2023).
23. Jingqiao, C. et al. Increased dysfunctional and plastic regulatory T cells in idiopathic orbital inflammation. *Front. Immunol.* <https://doi.org/10.3389/fimmu.2021.634847> (2021).
24. Yaping, F. et al. Composition and diversity analysis of the TCR CDR3 repertoire in patients with idiopathic orbital inflammation using high-throughput sequencing. *BMC Ophthalmol.* <https://doi.org/10.1186/s12886-023-03248-x> (2023).
25. Rebecca, V. What is ulcerative colitis? *JAMA* <https://doi.org/10.1001/jama.2023.23814> (2024).
26. Rashmi, K. S., David, B. B. & Katherine, R. C. Clonal hematopoiesis, inflammation, and hematologic malignancy. *Annu. Rev. Pathol.-Mech. Dis.* <https://doi.org/10.1146/annurev-pathmechdis-051222-122724> (2024).
27. Jane, A. B. G. & Gerald, J. H. Case report: Idiopathic sclerosing orbital inflammation. *Optometry Vis. Sci.* <https://doi.org/10.1097/oxp.0000000000001667> (2021).
28. Monaghan, T. M. et al. Orbital inflammatory complications of crohn's disease: A rare case series. *Clin. Med. Insights Gastroenterol.* **11**, 1179552218757512. <https://doi.org/10.1177/1179552218757512> (2018).
29. Angeline, F. M., Amina, I. M., Patricia, C.-B., Stacy, V. S. & Andrew, G. L. Idiopathic orbital inflammation associated with relapsing polychondritis. *Ophthalmic Plastic Reconstr. Surg.* <https://doi.org/10.1097/iop.0000000000000667> (2017).
30. Bram, V. et al. Sphingosine 1-phosphate modulation and immune cell trafficking in inflammatory bowel disease. *Nat. Rev. Gastroenterol. Hepatol.* <https://doi.org/10.1038/s41575-021-00574-7> (2022).
31. Delphine, O. et al. Risk factors leading to anti-TNF alpha therapies in pediatric severe uveitis. *Front. Pediatr.* <https://doi.org/10.3389/fped.2022.802977> (2022).
32. Leclercq, M. et al. Anti-tumor necrosis factor α versus tocilizumab in the treatment of refractory uveitic macular edema. *Ophthalmology* <https://doi.org/10.1016/j.ophtha.2021.11.013> (2022).
33. Yashawini, K. et al. TNF is a critical cytokine in age-related dry eye disease. *Ocular Surface* <https://doi.org/10.1016/j.jtos.2023.08.004> (2023).
34. Tao, J., Luqman, B., Altaf, D. & Naser, K. S2735 induction of inflammatory bowel disease by interleukin-17 inhibitor. *Am. J. Gastroenterol.* <https://doi.org/10.14309/01.ajg.0000867580.65574.96> (2022).
35. Zhou, H. F. et al. Quercetin serves as the major component of Xiang-lian Pill to ameliorate ulcerative colitis via tipping the balance of STAT1/PPAR γ and dictating the alternative activation of macrophage. *J. Ethnopharmacol.* **313**, 116557. <https://doi.org/10.1016/j.jep.2023.116557> (2023).
36. Elhefnawy, E. A., Zaki, H. F., El Maraghy, N. N., Ahmed, K. A. & Abd El-Haleim, E. A. Genistein and/or sulfasalazine ameliorate acetic acid-induced ulcerative colitis in rats via modulating INF- γ /JAK1/STAT1/IRF-1, TLR-4/NF- κ B/IL-6, and JAK2/STAT3/COX-2 crosstalk. *Biochem. Pharmacol.* **214**, 115673. <https://doi.org/10.1016/j.bcp.2023.115673> (2023).
37. Xie, F., Zhang, H., Zheng, C. & Shen, X. F. Costunolide improved dextran sulfate sodium-induced acute ulcerative colitis in mice through NF- κ B, STAT1/3, and Akt signaling pathways. *Int. Immunopharmacol.* **84**, 106567. <https://doi.org/10.1016/j.intimp.2020.106567> (2020).
38. Andújar, I. et al. Inhibition of ulcerative colitis in mice after oral administration of a polyphenol-enriched cocoa extract is mediated by the inhibition of STAT1 and STAT3 phosphorylation in colon cells. *J. Agric Food Chem.* **59**, 6474–6483. <https://doi.org/10.1021/jf2008925> (2011).
39. Li, Y. et al. STAT1, STAT6 and adenosine 3',5'-cyclic monophosphate (cAMP) signaling drive SOCS3 expression in inactive ulcerative colitis. *Mol. Med.* **18**, 1412–1419. <https://doi.org/10.2119/molmed.2012.00277> (2012).
40. García, L. N. et al. P022 Transcriptional biomarkers for vedolizumab therapy response in patients with moderate to severe Ulcerative Colitis. *J. Crohn's Colitis* <https://doi.org/10.1093/ecco-jcc/jjab232.151> (2022).
41. Masaru, T. et al. Elevated serum levels of CXCL9/monokine induced by interferon- γ and CXCL10/interferon- γ -inducible protein-10 in ocular sarcoidosis. *Investig. Ophthalmol. Visual Sci.* <https://doi.org/10.1167/iovs.05-0966> (2006).
42. Zemba, M. et al. Biomarkers of ocular allergy and dry eye disease. *Roman. J. Ophthalmol.* <https://doi.org/10.22336/rjo.2023.42> (2023).
43. Young Joon, C., Daehan, L., Suk Ho, B., Eui-Cheol, S. & Hyewon, C. Chemokine receptor profiles of T cells in patients with age-related macular degeneration. *Yonsei Med. J.* <https://doi.org/10.3349/ymj.2022.63.4.357> (2022).
44. Sujal, G. et al. Extended clinical and immunological phenotype and transplant outcome in CD27 and CD70 deficiency. *Blood* <https://doi.org/10.1182/blood.202006738> (2020).
45. Jun, C. et al. Active participation of antigen-nonspecific lymphoid cells in immune-mediated inflammation. *J. Immunol.* <https://doi.org/10.4049/jimmunol.177.5.3362> (2006).
46. Elizabeth, B., Eamonn Martin, Q. & Fergus, S. S1709 control of toll-like receptor (TLR) signalling in inflammatory bowel disease (IBD): Differential expression of key regulators of TLRs in ulcerative colitis (UC) and Crohn's disease (CD). *Gastroenterology* [https://doi.org/10.1016/s0016-5085\(09\)61155-0](https://doi.org/10.1016/s0016-5085(09)61155-0) (2009).
47. Weitaio, H., Taiyong, F. & Xiaoqing, C. Identification of differentially expressed genes and miRNAs for ulcerative colitis using bioinformatics analysis. *Front. Genet.* <https://doi.org/10.3389/fgene.2022.914384> (2022).
48. Chathyan, P. et al. Reduced CD27-IgD $^{+}$ B cells in blood and raised CD27-IgD $^{+}$ B cells in gut-associated lymphoid tissue in inflammatory bowel disease. *Front. Immunol.* <https://doi.org/10.3389/fimmu.2019.00361> (2019).
49. Jun, H., Zhi-Jie, N. & Zhongbo, L. Intercellular adhesion molecule 1 and selectin I play crucial roles in ulcerative colitis. *Medicine* <https://doi.org/10.1097/md.0000000000003652> (2023).

50. Hu, J., Zhou, S. & Guo, W. Construction of the coexpression network involved in the pathogenesis of thyroid eye disease via bioinformatics analysis. *Hum. Genomics* **16**, 38. <https://doi.org/10.1186/s40246-022-00412-0> (2022).
51. Liu, H. et al. Identification of hub genes associated with nonspecific orbital inflammation by weighted gene coexpression network analysis. *Dis. Markers* **2022**, 7588084. <https://doi.org/10.1155/2022/7588084> (2022).
52. Wang, W. et al. Shared biomarkers and immune cell infiltration signatures in ulcerative colitis and nonalcoholic steatohepatitis. *Sci. Rep.* **13**, 18497. <https://doi.org/10.1038/s41598-023-44853-6> (2023).

Author contributions

Kang Tan and Zixuan Wu drafted and revised the manuscript, Pei Liu and Zixuan Wu were in charge of data collection, Xi Long and Yufeng Yu were in charge of the design of the frame, Qinghua Peng and Pengfei Jiang conceived and designed this article, in charge of syntax modification and revision of the manuscript.

Funding

Financial support was provided by the National Natural Science Foundation of China (No. 81574031); Key Project of Scientific Research Fund of Hunan Provincial Department of Education (No. 21A0238, No. 22A0241, No. 22B0374); Natural Science Foundation of Hunan Province (No. 2023JJ40479).

Declarations

Competing interests

The authors declare no competing interests.

Ethics approval and consent to participation

This manuscript is not a clinical trial, hence the ethics approval and consent to participation are not applicable.

Consent for publication

All authors have read and approved this manuscript to be considered for publication.

Additional information

Supplementary Information The online version contains supplementary material available at <https://doi.org/10.1038/s41598-025-89344-y>.

Correspondence and requests for materials should be addressed to P.J. or Q.P.

Reprints and permissions information is available at www.nature.com/reprints.

Publisher's note Springer Nature remains neutral with regard to jurisdictional claims in published maps and institutional affiliations.

Open Access This article is licensed under a Creative Commons Attribution-NonCommercial-NoDerivatives 4.0 International License, which permits any non-commercial use, sharing, distribution and reproduction in any medium or format, as long as you give appropriate credit to the original author(s) and the source, provide a link to the Creative Commons licence, and indicate if you modified the licensed material. You do not have permission under this licence to share adapted material derived from this article or parts of it. The images or other third party material in this article are included in the article's Creative Commons licence, unless indicated otherwise in a credit line to the material. If material is not included in the article's Creative Commons licence and your intended use is not permitted by statutory regulation or exceeds the permitted use, you will need to obtain permission directly from the copyright holder. To view a copy of this licence, visit <http://creativecommons.org/licenses/by-nc-nd/4.0/>.

© The Author(s) 2025